Autonomous Fuzzy Parking Control of a Car-Like Mobile Robot

Tzuu-Hseng S. Li, *Member, IEEE,* and Shih-Jie Chang

***Abstract*—This paper is devoted to design and implement a car-like mobile robot (CLMR) that possesses autonomous garage-parking and parallel-parking capability by using real-time image processing. For fuzzy garage-parking control (FGPC) and fuzzy parallel-parking control (FPPC), feasible reference trajectories are provided for the fuzzy logic controller to maneuver the steering angle of the CLMR. We propose two FGPC methods and two FPPC methods to back-drive or head-in the CLMR to the garage and the parking lot, respectively. Simulation results illustrate the effectiveness of the developed schemes. The overall experimental setup of the parking system developed in this paper is composed of a host computer, a communication module, a CLMR, and a vision system. Finally, the image-based real-time implementation experiments of the CLMR demonstrate the feasibility and effectiveness of the proposed schemes.**

***Index Terms*—Car-like mobile robot, fuzzy logic control, garage parking, parallel parking, real-time implementation.**

I. Introduction

In RECENT years, autonomous parking problems [1]–[23] of the CLMR have attracted a great deal of attention from research organization and automobile industry. Basically, the parking problems can be classified into two categories: garage-parking problem and parallel-parking problem. The garage-parking [1]–[8], [22], [23] and parallel-parking [9]–[23] schemes have been examined in many papers in the literature. Most of these researches have been concentrated on tracking and posture stabilization methods. The tracking method is to design a control algorithm that makes a CLMR follow a reference trajectory. The posture stabilization method is to stabilize the CLMR to a desired final posture from any initial posture.

Sugeno and Murakami [1] propose an experimental study on FGPC using model car, which is equipped with on-board microprocessor and two supersonic sensors for the measurements of the relative distance and direction. They derive fuzzy control rules by utilizing Sugeno-type fuzzy implications to model the parking experience of a skilled driver. Sugeno *et al.* [2] adopt the similar hardware arrangement as that in [1] to execute the garage parking by employing fourteen fuzzy oral instructions such as "go straight," "slow down," "enter garage," and "speed up."

Manuscript received April 22, 2002; revised October 7, 2002. This work was supported by the National Science Council, Taiwan, R.O.C., under Grants NSC89-2213-E006-187, NSC90-2213-E006-052, and NSC91-2213-E006-026. This paper was recommended by Associate Editor D. Y. Lee.

The authors are with the IC^{2}S Laboratory, Department of Electrical Engineer, National Cheng-Kung University, Tainan 70101, Taiwan, R.O.C. (e-mail: thsli@mail.ncku.edu.tw).

Digital Object Identifier 10.1109/TSMCA.2003.811766

A nonlinear control proposed by Sampei and Furuta [3] for parking a car from any position to an appointed parking position is studied through trajectory simulations. The simulation results of the nonlinear control illustrate the best convergence compared with a LQ regulator and a human model control, which is based on Kondo's driver model. The car can be guided along the minimum pass with parking problem by this control combined with changing a straight guideline. Yasunobu and Murai [4] exploit the state evaluation fuzzy control and the predictive fuzzy control to achieve the drive knowledge. Only the computer simulations are given to show the effectiveness of the proposed parking control.

A skilled-based visual parking control using neural networks and fuzzy is discussed in [5], where two control architectures, the direct neural control and the fuzzy hybrid control, are used to generate the automatic parking commands. The environment information is measured by a video sensor. The control architectures are validated by experiments with an autonomous mobile robot. Tayebi and Rachid [6] deal with the parking problem of CLMR by using time-varying state feedback control law via the Lyapunov direct method. The control law is robust to ensure a global boundedness of the system states under measurement perturbations.

The development of a near-optimal fuzzy controller for maneuvering a car in a parking lot is described in [7]. A cell mapping based method is proposed to systematically group near-optimal trajectories for all possible initial states in the parking lot. The rules and membership functions of the fuzzy controller are generated using the statistical properties of the individual trajectory groups. An *et al.* [8] develop an online path-planning algorithm that guides an autonomous mobile robot to a goal with avoiding obstacles in an uncertain world. The established autonomous mobile robot cannot move omni-direction and run on two wheels equipped with a CCD camera. The path-planning algorithm is constructed by three modes: straight mode, spin mode, and avoidance mode. The simulation program and experimental results are developed to check this algorithm by using the garage parking motion.

Shirazi and Yih [9] propose an expert's knowledge including symbolic form and nonsymbolic form, where the former can be obtained from expert directly and the latter can be obtained only through an evolutionary process. The evolutionary process consists of three stages: novice, competency, and expert. The developed intelligent control system performs parallel parking to show validity and ability. The fuzzy traveling control of an autonomous mobile robot with six supersonic sensors has been provided in [10], where the flush problem are considered.

The parallel-parking problem of curvilinear path generation for a car with nonholonomic constraints is proposed in [11]. A fifth-order polynomial as the parallel-parking path is derived by utilizing slope and curvature constraints. The relationship between the rear-path curvature and the steering angle is also developed. Murray and Sastry [12] propose a method for open-loop steering of nonholonomic systems by using sinusoidal trajectory which are optimal input form in chained system.

A complete motion-planning scheme for a CLMR is developed in [13]. That has three stages:

1) plan a path for the geometric system;
2) perform a subdivision on the path until all endpoints can be linked by optimal feasible paths;
3) run an "optimization" routine to reduce the length of the path.

The scheme has been implemented in a complex environment including a number of polygonal obstacles. Paromtchik and Laugire [14] propose an iterative parallel-parking algorithm for a nonholonomic vehicle with ultrasonic sensor system, where the vehicle follows sinusoidal reference functions.

Laugier *et al.* [15] propose a novel control architecture for a car-like vehicle with dynamic moving. The control architecture includes an offline global trajectory planner, a decisional kernel which generates on-line appropriate senor-based manoeuvres, and a motion controller. Two experiment results of lane following/changing and parallel parking are presented with a real automatic car. A genetic algorithm (GA) based on fuzzy control is set up in [16], where they exploit a new context-dependent coding technique, a chromosome reordering operator, and the coevolution of controller testing sets to improve the conventional GAs in designing controller. The algorithm is applied to parallel parking maneuver for mobile robots.

An abstraction mechanism based on flows of commutators of vector fields is formulated in [17] and is applied to the goal-directed motion of a car and the standard path-planning algorithm. Lian *et al.* [18] investigate a fuzzy gain scheduling controller to parallel park a CLMR, where a fuzzy sliding mode controller is firstly used to locally track a typical path for the parallel parking. For the nonholonomic constraints and mechanical constraints, several typical paths are formed to complete the parallel parking procedure. Jiang [19] and [20] offers an automated parking system works in three phases, scanning, positioning, and manoeuvring. Speed control during the manoeuvre is also discussed. A real-time collision-free path algorithm is designed the basis of mathematical models. The experiments of the parking system have been presented on a B12 mobile robot with embedded microprocessor with ultrasonic sensors.

A motion planning for autonomous parking of an intelligent vehicle by utilizing vision is proposed in [21], where color segmentation method is based on RCE neural network. They apply quintic polynomials and symmetric posture to provide good results in local path planning for automatic parking behaviors. Autonomous parking algorithm is implemented in a simulation program and a real Smart Car. Gorinevsky *et al.* [22] explore stability of feedback controller, and optimal trajectory planning and formulation for parking problem. A parking motion planning architecture based on a radial basis function network is also presented. Two general cases of backward parking are emulated by using the proposed controller.

The parking problem with the point-stabilization problem of nonholonomic CLMR is investigated in [23]. The algorithm is divided in two steps: stabilization to a desired line and stabilization to desired point. The steering operation is determined by nonlinear state feedback control law. Simulations and experiments using a CLMR, Postur-I, verify the performance of the algorithm.

Generally speaking, the kinematics equations of a car with nonholonomic constraints are nonlinear and time-varying differential equations. It is almost impossible to find an auto-driver by a traditional control method to maneuver the car to perform the garage parking or parallel parking. However, a human driver can smoothly and even perfectly park the car into garage or parking zone by some simple instinct rules without the knowledge of the motion kinematics of the automobile.

It is well known that fuzzy set theory is arisen from the desire of linguistic description for complex system and it can be utilized to formulate and translate the human experience to appropriately automatic control strategies. This kind of human intelligence is easily represented by the fuzzy logic control structure. Most advanced control algorithms in autonomous mobile robots can benefit from fuzzy logic control.

Among these literatures [1]–[23], one can find that about half the garage parking and the parallel parking are maneuvered by the fuzzy logic control (FLC) scheme. In fact, the FLC has been successfully applied to numerous industrial appliances, consumer electronics, and autonomous mobile robots. The decision-making logic (DML) rules of a FLC can be obtained from human experts, learning mechanisms, evolution algorithms, or some traditional control theories. The parking problem that will be dealt with in this paper corresponds to a reference trajectory tracking, and we will propound two FGPC methods and two FPPC methods for the CLMR in the coordinate systems. The DML rules are derived by the sliding-mode control and human driving skills.

This paper is organized as follows. In Section II, for back-drive and head-in parking, kinematic equations and reference trajectories for garage parking and parallel parking are derived. Suitable FGPC and FPPC are investigated such that a CLMR can park in the desired zone appropriately and automatically in Section III. Computer simulation results are given to show the validity of the proposed fuzzy logic control algorithms. Section IV addresses the overall system architecture of the CLMR, where the host computer, communication module, the CLMR, and vision system are presented. The image-based real-time parking controls of the CLMR are also presented in this section. Two FGPC schemes and two FPPC schemes are all applied to implement the real-time garage parking and the real-time parallel parking, respectively. Section V concludes this paper.

II. Kinematic Equations and Reference Trajectories

The motion of the CLMR is discussed firstly in this section. Two kinds of kinematic equations for CLMR are examined and

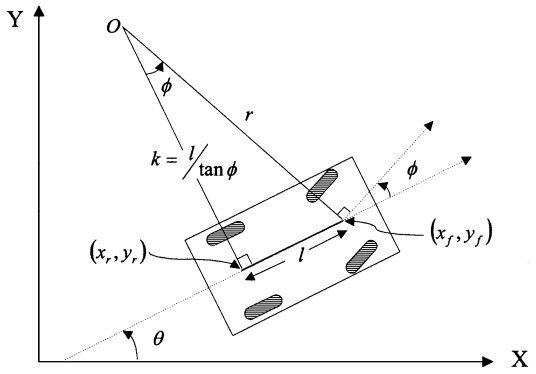

Fig. 1. Kinematic model of a CLMR.

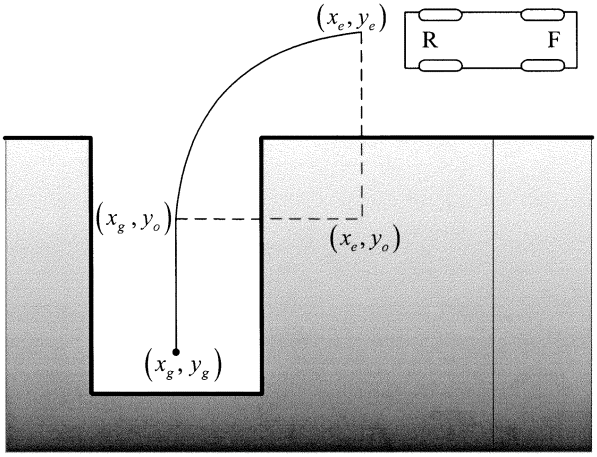

Fig. 2. Reference trajectories for backward garage parking.

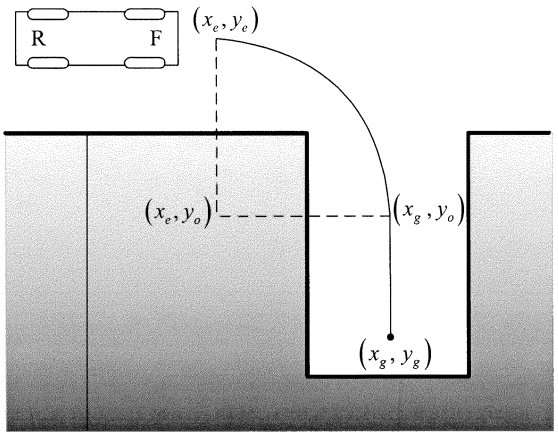

Fig. 3. Reference trajectories for forward garage parking.

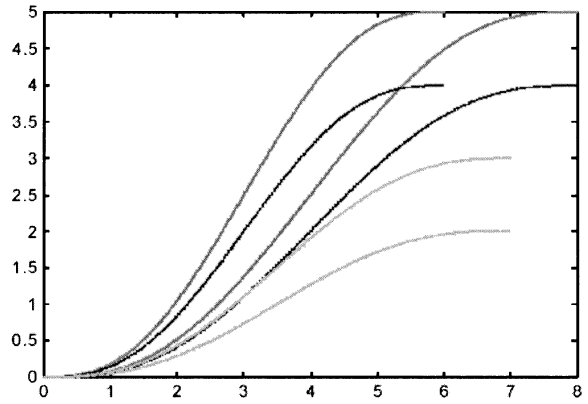

Fig. 4. Reference trajectories of the fifth-order polynomial with six initial locations (x_e, y_e): (8, 5), (8, 4), (7, 3), (7, 4), (6, 5), and (6, 4).

reference trajectories for garage parking and parallel parking are then provided.

A. Modeling of a CLMR

Consider a kinematic model of the CLMR shown in Fig. 1, where the rear wheels are fixed parallel to car body and allowed to roll or spin but not slip. The front wheels can turn to left or right, but the left and right front wheels must be parallel. All the corresponding parameters of the CLMR depicted in Fig. 1 are defined as follows.

(x_f, y_f)	position of the front wheel center of CLMR;
(x_r, y_r)	position of the rear wheel center of CLMR;
ϕ	orientation of the steering-wheels with respect to the frame of CLMR;
θ	angle between vehicle frame orientation and X-axis;
l	wheel-base of CLMR;
O	center of curvature;
r	distance from point O to point (x_f, y_f);
k	curvature of the fifth-order polynomial.

The rear wheel is always tangent to the orientation of the vehicle. The no-slipping condition mentioned previously requires that the CLMR travels in the direction of its wheels. Thus, we have

$$\dot{y}_r \cos\theta - \dot{x}_r \sin\theta = 0. \tag{1}$$

This is the so-called nonholonomic constraint. The front of the CLMR is fixed relative to the rear, thus the coordinate (x_r, y_r) is related to (x_f, y_f)

$$\begin{aligned} x_r &= x_f - l\cos\theta \\ y_r &= y_f - l\sin\theta. \end{aligned} \tag{2}$$

Thus, differentiating (2) with respect to time gives

$$\begin{aligned} \dot{x}_r &= \dot{x}_f + \dot{\theta} l \sin\theta \\ \dot{y}_r &= \dot{y}_f - \dot{\theta} l \cos\theta. \end{aligned} \tag{3}$$

Substituting (3) to (1), we can get

$$\dot{x}_f \sin\theta - \dot{y}_f \cos\theta + \dot{\theta} l = 0. \tag{4}$$

From Fig. 1, we have

$$\begin{aligned} \dot{x}_f &= \nu \cdot \cos(\theta + \phi) \\ \dot{y}_f &= \nu \cdot \sin(\theta + \phi). \end{aligned} \tag{5}$$

Substituting (5) to (4), we can derive

$$\dot{\theta} = \nu \cdot \frac{\sin\phi}{l}. \tag{6}$$

Equations (5) and (6) are the kinematic equations of CLMR with respect to the axle center of the front wheels. We rewrite them in the following:

$$\begin{aligned} \dot{x}_f &= \nu \cdot \cos(\theta + \phi) \\ \dot{y}_f &= \nu \cdot \sin(\theta + \phi) \\ \dot{\theta} &= \nu \cdot \frac{\sin\phi}{l}. \end{aligned} \tag{7}$$

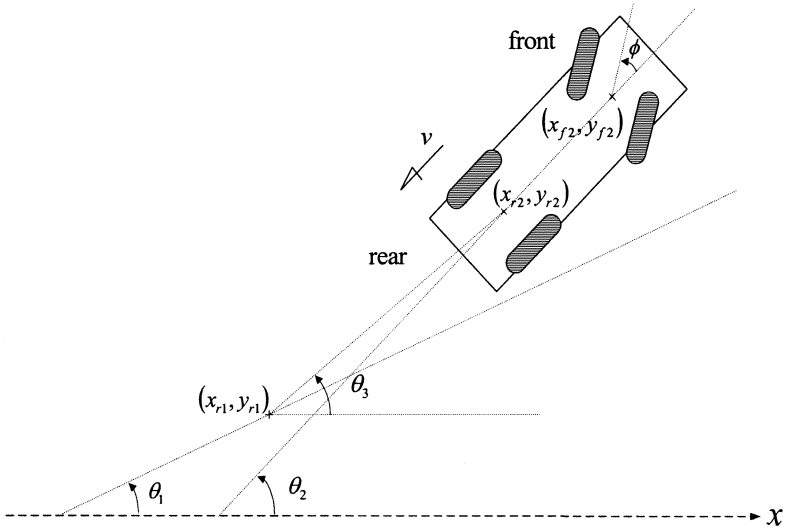

Fig. 5. Definition of parameters for backward FGPC.

Equations (7) are used to generate the next forward state position of the vehicle when the present states and control input are given. Following these equations describing the motion kinematics, we can easily obtain the kinematic equations of the vehicle motion described by the position of the front wheel center (x_r, y_r). Then we can apply (3) to (7), the kinematics of CLMR with respect to the axle center of the rear wheels will be described as

$$\begin{aligned} \dot{x}_r &= \nu \cdot \cos\theta\cos\phi \\ \dot{y}_r &= \nu \cdot \sin\theta\cos\phi \\ \dot{\theta} &= \nu \cdot \frac{\sin\phi}{l}. \end{aligned} \tag{8}$$

Equations (8) are used to generate the next backward state position of the vehicle when the present state and control input are given.

B. Reference Trajectories for Garage Parking

Traditionally, a path planner who takes into account of the environmental model as well as the vehicle's dynamics and constraints determines a reference trajectory. It is important for us to provide reasonable reference trajectories such that the CLMR can successfully accomplish the garage-parking mission. If the reference trajectory is far from a feasible one because of the unmodeled dynamics or modeling inaccuracy, then the vehicle is unable to follow the trajectory accurately. To avoid the abnormality, we must adopt a precise reference trajectory to track. To evaluate the feasibility and effectiveness of FGPC scheme, we set up two test grounds for garage parking—backward garage parking and forward garage parking.

By backward garage parking, according to our driving experiences, we always turn the steering wheel to the right and back the car. Then the car will result in an arc trajectory as entering the garage. Thus, a quarter circle is used to form this trajectory. Because we hope the car can keep backing straight in the garage, we draw a line at the end of the quarter circle as a desired path. In other words, the reference trajectory for backward garage parking includes a circular motion and a straight-line motion. Fig. 2 shows the proposed trajectory, where (x_e, y_o) is the virtual center of the circle, (x_g, y_o) is the connection point, (x_e, y_e) is the initial location of the reference trajectory, and (x_g, y_g) is the final location for (x_r, y_r).

The reference rear trajectory during backward garage parking is represented as a function $y_r = f(x_r)$. The general form for circular motion is given by

$$(x_r - x_e)^2 + (y_r - y_o)^2 = (x_e - x_g)^2. \tag{9a}$$

And the line motion becomes

$$x_r = x_g \quad \text{and} \quad y_g \le y_r \le y_0. \tag{9b}$$

If the vehicle can follow this reference trajectory completely, one can definitely say that the vehicle parks in the garage correctly.

Suppose the garage is wide enough to park the vehicle directly, we could design a controller such that the vehicle can move forward into the garage. The corresponding reference trajectory is shown in Fig. 3. The reference front trajectory during forward garage parking is represented as a function $y_f = f(x_f)$. The general form for circular motion is now given by

$$(x_f - x_e)^2 + (y_f - y_o)^2 = (x_g - x_e)^2. \tag{10a}$$

And the line motion now is

$$x_r = x_g \quad \text{and} \quad y_g \le y_r \le y_0. \tag{10b}$$

The idea of forward garage parking is the same as that of backward garage parking. Similarly, if the vehicle can follow this reference trajectory completely, we would say that the CLMR can park in the garage correctly.

C. Reference Trajectories for Parallel Parking

In order to implement the parallel parking, we adopt a feasible and smooth trajectory [11] such that the CLMR can track. In fact, several curves have been used to present the reference trajectory such as two circular arcs, sine curve, cosine curve, and a fifth-order polynomial curve etc. These curves are determined by the initial position of the CLMR and final position of parking zone. Lyon [11] has shown that a fifth-order polynomial is the least polynomial behaving the parallel parking. Moreover,

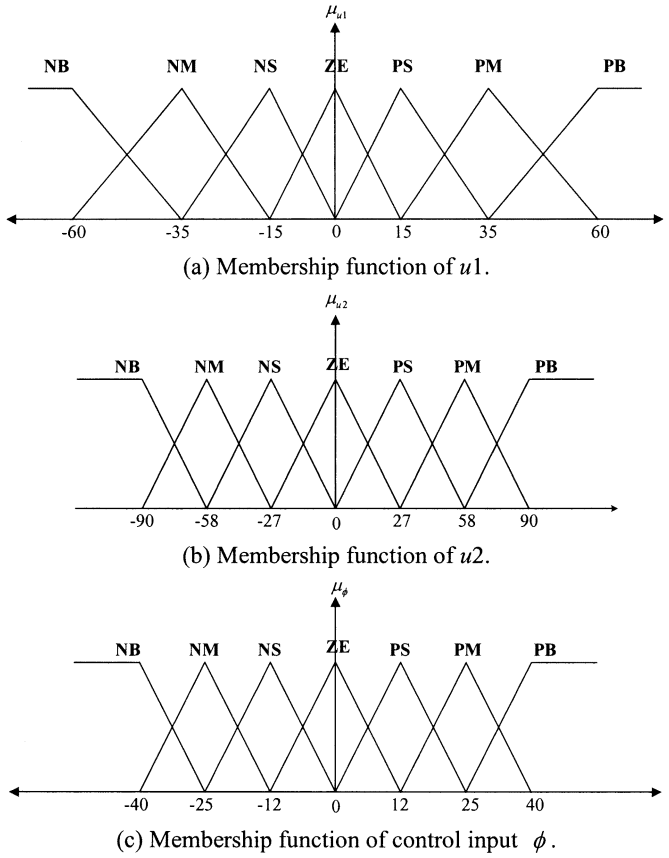

Fig. 6. Fuzzy membership functions for the input–output variables.

compared with the fifth-order polynomial, the disadvantage of those simple curves is that they induce an extra time penalty in straightening out the wheel at the maneuver end-points. The detail derivation of the fifth-order reference trajectory is examined as follows.

The reference trajectory for backward parallel parking is represented as a function $y_r = f(x_r)$. The general form of a fifth-order polynomial is given by [11]

$$y_r(x_r) = a_5\left(\frac{x_r}{x_e}\right)^5 + a_4\left(\frac{x_r}{x_e}\right)^4 + a_3\left(\frac{x_r}{x_e}\right)^3 + a_2\left(\frac{x_r}{x_e}\right)^2 + a_1\left(\frac{x_r}{x_e}\right) + a_0 \tag{11a}$$

$$y_r'(x_r) = \frac{5a_5}{x_e}\left(\frac{x_r}{x_e}\right)^4 + \frac{4a_4}{x_e}\left(\frac{x_r}{x_e}\right)^3 + \frac{3a_3}{x_e}\left(\frac{x_r}{x_e}\right)^2 + \frac{2a_2}{x_e}\left(\frac{x_r}{x_e}\right) + \frac{x_r}{x_e} \tag{11b}$$

$$y_r''(x_r) = \frac{20a_5}{x_e^2}\left(\frac{x_r}{x_e}\right)^3 + \frac{12a_4}{x_e^2}\left(\frac{x_r}{x_e}\right)^2 + \frac{6a_3}{x_e^2}\left(\frac{x_r}{x_e}\right) + \frac{2a_2}{x_e^2} \tag{11c}$$

where (x_e, y_e) is the initial location of the polynomial. The constraints on slope of (11) are

$$y_r' = \frac{dy_r}{dx_r}, \quad y_r'(0) = y_r'(x_e) = 0. \tag{12}$$

The curvature at the end points satisfies

$$k(0) = k(x_e) \tag{13}$$

TABLE I
FUZZY RULE TABLE FOR BACKWARD FGPC

u1 \ u2	NB	NM	NS	ZE	PS	PM	PB
NB	ZE	NS	NM	NB	NB	NB	NB
NM	PS	ZE	NS	NM	NB	NB	NB
NS	PM	PS	ZE	NS	NM	NB	NB
ZE	PB	PM	PS	ZE	NS	NM	NB
PS	PB	PB	PM	PS	ZE	NS	NM
PM	PB	PB	PB	PM	PS	ZE	NS
PB	PB	PB	PB	PB	PM	PS	ZE

TABLE II
FUZZY RULE TABLE FOR FORWARD FGPC

u1 \ u2	NB	NM	NS	ZE	PS	PM	PB
NB	ZE	PS	PM	PB	PB	PB	PB
NM	NS	ZE	PS	PM	PB	PB	PB
NS	NM	NS	ZE	PS	PM	PB	PB
ZE	NB	NM	NS	ZE	PS	PM	PB
PS	NB	NB	NM	NS	ZE	PS	PM
PM	NB	NB	NB	NM	NS	ZE	PS
PB	NB	NB	NB	NB	NM	NS	ZE

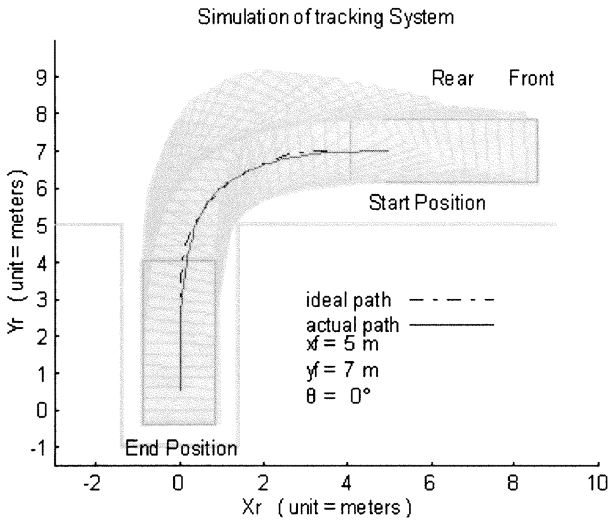

Fig. 7. Simulation result of backward garage parking: vehicle with start posture $(x_{r2}, y_{r2}, \theta) = (5, 7, 0^\circ)$.

where

$$k(x_r) = \frac{y_r''}{\left[1 + (y_r')^2\right]^{\frac{3}{2}}} \tag{14}$$

so that

$$y_r''(0) = y_r''(x_e) = 0. \tag{15}$$

We can obtain the reference trajectory as

$$y_r(x_r) = y_e\left[6\left(\frac{x_r}{x_e}\right)^5 - 15\left(\frac{x_r}{x_e}\right)^4 + 10\left(\frac{x_r}{x_e}\right)^3\right]. \tag{16}$$

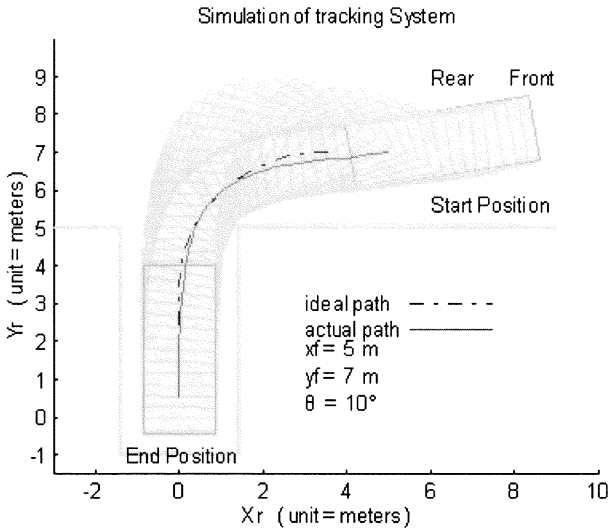

Fig. 8. Simulation result of backward garage parking: vehicle with start posture $(x_{r2}, y_{r2}, \theta) = (5, 7, 10°)$.

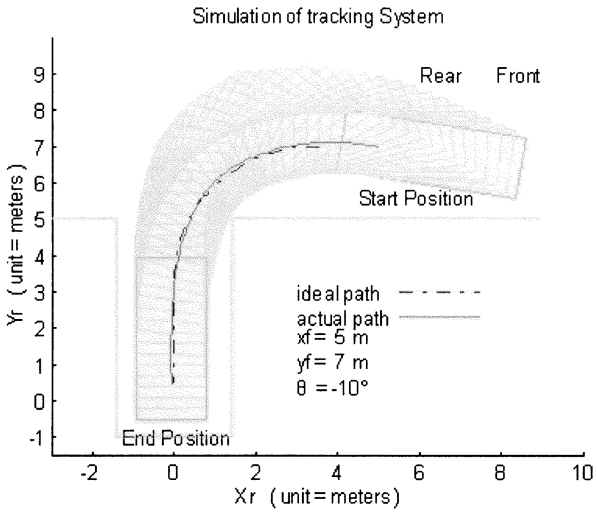

Fig. 9. Simulation result of backward garage parking: vehicle with start posture $(x_{r2}, y_{r2}, \theta) = (5, 7, -10°)$.

Substituting (16) into (14) results in

$$k(x_r) = \frac{y_e\left(120\frac{{x_r}^3}{{x_e}^5} - 180\frac{{x_r}^2}{{x_e}^4} + 60\frac{x_r}{{x_e}^3}\right)}{\left[1 + {y_e}^2\left(30\frac{{x_r}^4}{{x_e}^5} - 60\frac{{x_r}^3}{{x_e}^4} + 30\frac{{x_r}^2}{{x_e}^3}\right)^2\right]^{\frac{3}{2}}}. \quad (17)$$

Some different reference trajectories of the fifth-order polynomial are shown in Fig. 4, where there are six initial locations.

The reference front trajectory during forward parallel parking is also represented as a function $y_f = f(x_f)$. The general form of a fifth-order polynomial is now given by

$$y_f(x_f) = y_e\left[6\left(\frac{x_f}{x_e}\right)^5 - 15\left(\frac{x_f}{x_e}\right)^4 + 10\left(\frac{x_f}{x_e}\right)^3\right]. \quad (18)$$

If the vehicle can follow this reference trajectory completely, we would say that the CLMR could park in the parking zone correctly.

III. Fuzzy Parking Control Design

After providing the reference trajectories, we propose forward and backward parking methods for back-drive parking and head-in parking, respectively. We address the design procedures for the FGPC and FPPC. Computer simulations are also given to examine the feasibility.

A. Backward FGPC

The main theme of the backward FGPC is to make the CLMR follow the derived reference trajectory from the start position to the end position. The parameters used to construct the backward FGPC is shown in Fig. 5, where (x_{r1}, y_{r1}) is the desired position of the reference trajectory at some sampling instant, θ_1 is its orientation angle corresponding to the X-axis, the orientation angle of the CLMR is θ_2, and θ_3 denotes an orientation angle between the X direction and the line from (x_{r1}, y_{r1}) to (x_{r2}, y_{r2}). We adopt a two-input-single-output FLC for the garage-parking task.

It is well known that the rules of a FLC are usually determined by the human operator's behavior. In essence, a FLC is an algorithm that can convert the linguistic control strategy based on the knowledge of expert or operator into an automatic control strategy. The kernel of the FLC is a set of linguistic control rules. In this experiment, according to the parking skill in our daily life, fuzzy reasoning rules for the backward FGPC can be expressed in linguistic form as follows.

Let the input variable of the FGPC be defined as

$$u_1 = \theta_3 - \theta_1 \quad (19a)$$

$$u_2 = \theta_2 - \theta_1. \quad (19b)$$

The output linguistic variable is the steering angle ϕ. The membership functions of $u1$, $u2$ and ϕ are shown in Fig. 6, where they all are decomposed into seven fuzzy partitions, such as negative big (NB), negative medium (NM), negative small (NS), zero (ZE), positive small (PS), positive medium (PM), and positive big (PB). Since each input is divided into seven fuzzy sets, forty-nine fuzzy rules must be determined. We develop the backward FGPC by using the fuzzy sliding-mode control (FSMC) [24]–[26]. For FSMC, we first have to choose the sliding surface (in fact, the sliding line in this application) that represents the control purpose. For instance, the sliding line is defined as

$$s = u1 - u2. \quad (20)$$

Substituting the definition of $u1$ and $u2$ into (20) implies

$$s = \theta_3 - \theta_2. \quad (21)$$

Suppose $s = 0$, i.e., $\theta_3 = \theta_2$, which presents that the CLMR follows the trajectory, then the steering angle ϕ should be zero. One of the corresponding linguistic meanings is that "if $u1$ is NB and $u2$ is NB, then ϕ is ZE." Similar ϕ can be determined when $u1$ and $u2$ are in NM, NS, . . ., PB. Suppose $s < 0$, (for example, $u1$ is NS and $u2$ is PS), this phenomenon denotes the CLMR is just above the desired trajectory, we have to turn the steering angle to the left to increase θ_3 and decrease θ_2. Similarly, if $u1$ is NB and $u2$ is PB, then ϕ should be NB. On the other hand, if $s > 0$, then $\phi > 0$. We can conclude that if $u1 - u2$ is closed to the sliding line, the control action is smaller than those are far from the line. The rule table for backward garage parking is summarized in Table I. The defuzzification strategy is the center of area method.

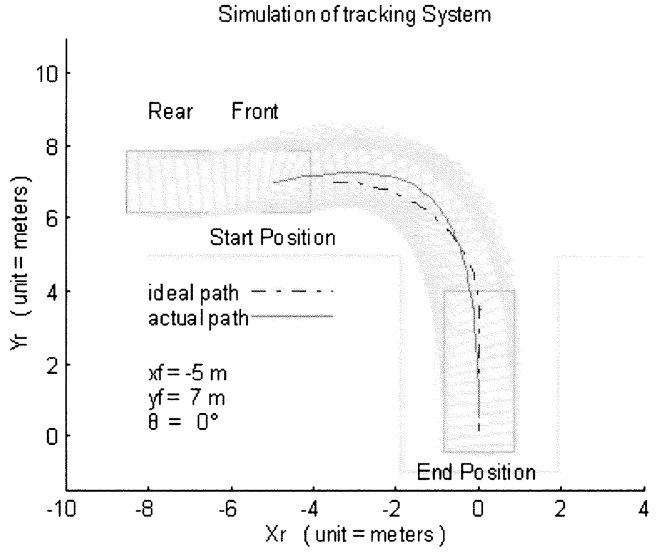

Fig. 10. Simulation result of forward garage parking: vehicle with start posture $(x_{f2}, y_{f2}, \theta) = (-5, 8, 0^\circ)$.

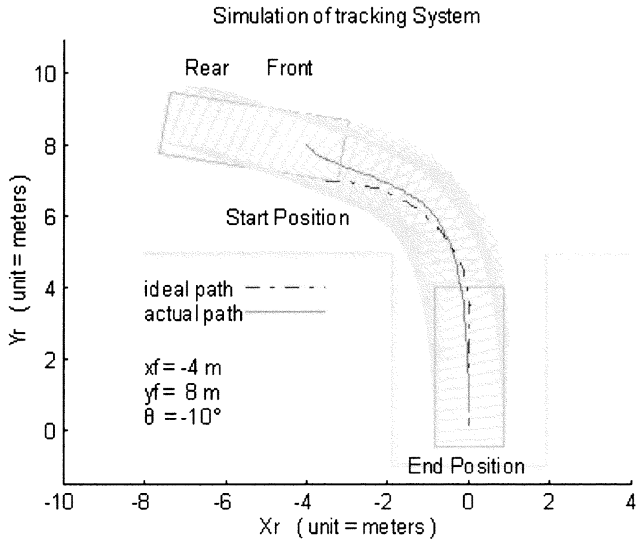

Fig. 11. Simulation result of forward garage parking: vehicle with start posture $(x_{f2}, y_{f2}, \theta) = (-4, 8, -10^\circ)$.

B. Forward FGPC

The CLMR can track a reference trajectory and accomplish the garage-parking problem in forward FGPC scheme. In this case, the kinematic equation of the CLMR is represented by (7). The reference trajectory for forward garage parking is described in (10) except the start position (x_e, y_e) is located at the second quadrant, i.e., $x_e < 0$ and $y_e > 0$. Except the fuzzy rule table, all the parameters and settings of the forward FGPC are the same as those in the backward one. The fuzzy rule table for forward FGPC is listed in Table II, which is skew-symmetric to Table I. Now, we take one rule to explain. The rule: "if $u1$ is NS and $u2$ is PS, then ϕ is PM" represents that the CLMR is above the ideal trajectory, one should turn the steering angle to the right with a medium force to go along the trajectory.

C. Simulation Results for FGPC

The computer simulation results of the CLMR are given to demonstrate the effectiveness of the proposed control schemes. Taking account of real life, the length of the garage is about 1.5 times longer than that of the car, and the widths of the garage are 1.5 and 2 times wider than that of the car for back-drive and head-in garage parking, respectively. That is why the setup of test ground for forward garage parking is wider than that of backward one.

The CLMR used in the simulation has the following dimensions: length $L = 4.45$ m, width $W = 1.695$ m, and wheel base $l = 2.62$ m. For backward garage parking, garage has the dimensions: garage length 6.675 m and garage width 2.54 m. For forward garage parking, garage has the dimensions: garage length 6.675 m and garage width 3.4 m. We exploit the following cases with several situations to test the effectiveness of the proposed FGPC scheme.

For backward garage parking, the reference trajectory starts with the initial location $(x_e, y_e) = (3.5, 7.0)$ with orientation 0° and ends at the final location (0, 0) with orientation 90°. Suppose the start postures of the CLMR are located at $(x_{r2}, y_{r2}, \theta_2) = (5, 7, 0^\circ)$,(5, 7, 10°), and (5, 7, -10°)

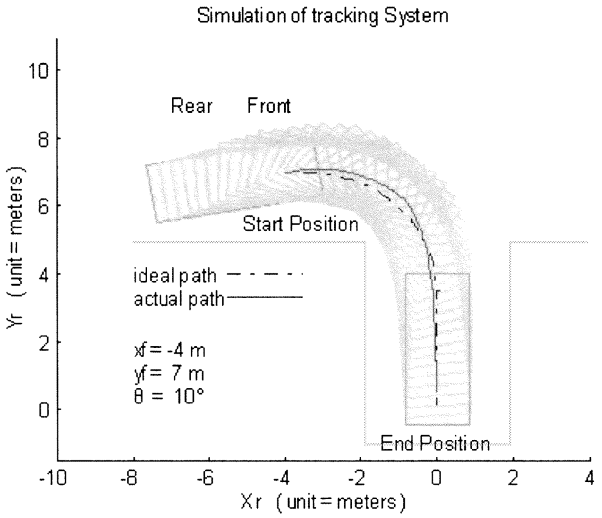

Fig. 12. Simulation result of forward garage parking: vehicle with start posture $(x_{f2}, y_{f2}, \theta) = (-4, 7, 10^\circ)$.

respectively. Simulation results for these three start postures are illustrated in Figs. 7, and 8, and 9, respectively. For forward garage parking, the reference trajectory starts with the initial location $(x_e, y_e) = (-3.5, 7.0)$ with orientation 0° and ends at the finial location (0, 0) with orientation -90°. Suppose the start postures of the CLMR are located at $(x_{f2}, y_{f2}, \theta_2) = (-3, 8, 0^\circ)$, (− 4, 8, -10°), and (− 4, 7 -10°, respectively, then the simulation results for these three start postures are illustrated in Figs. 10, 11, and 12.

We can find that the less differences between the initial posture of the reference trajectory and the start posture of the CLMR, the less differences between the ides path and the actual path. It is also seen very clearly from all these figures that we successfully control the vehicle to park at the desired position.

D. Backward FPPC

To make the CLMR follow backwardly the derived reference trajectory from the start position to the end position is the pur-

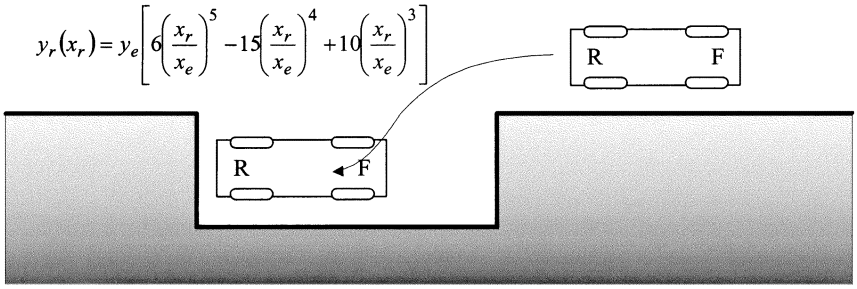

Fig. 13. Backward parallel parking.

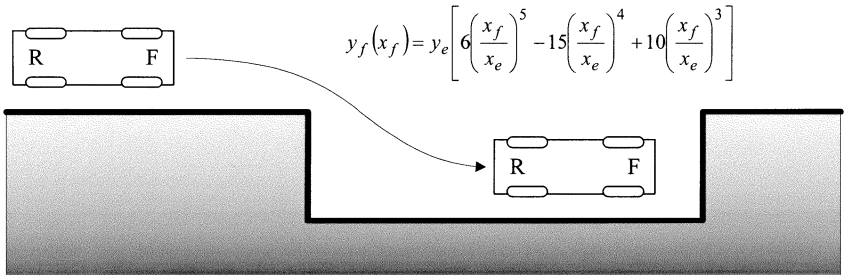

Fig. 14. Forward parallel parking.

pose of the backward FPPC. In this case, the kinematic equation of the CLMR is represented by (8). The fifth-order polynomial of the reference trajectory is described in (16). Fig. 13 illustrates the reference trajectory of the backward parallel parking. Similarly, the fuzzy variable and the fuzzy inference rules for the backward FPPC are the same as those in backward FGPC and the descriptions are omitted here for the sake of saving the paper length.

E. Forward FPPC

The main objective in this subsection is to design a FPPC scheme such that the CLMR can track forwardly a reference trajectory and accomplish the parallel-parking problem. In this case, the dynamic equation of the CLMR is represented by (7). The fifth-order polynomial of the reference trajectory is the same as that in (18) except the start position (x_e, y_e) is located at the second quadrant, i.e., $x_e < 0$ and $y_e > 0$. The reference trajectory of the forward parallel parking is shown Fig. 14. All the parameters, settings, and the fuzzy rule table of the forward FPPC are also the same as those in the forward FGPC.

F. Simulation Results for FPPC

The dimensions of the CLMR used in the simulation are the same as those in FGPC. According real life, the width of the parking zone is about 1.5 times wider than that of the car, the lengths of the parking zone are 1.5 and 1.8 times longer than that of the car for back-drive and head-in parallel parking, respectively. Similarly, the setup of test ground for forward parallel parking is longer than that of backward one.

The parking zone has the dimensions as follows. The width of the parking zone is 2.54 m. But, for backward parallel parking, the length of the parking zone is 6.675 m; for forward parallel parking, the length of the parking zone is 8.9 m. We also exploit

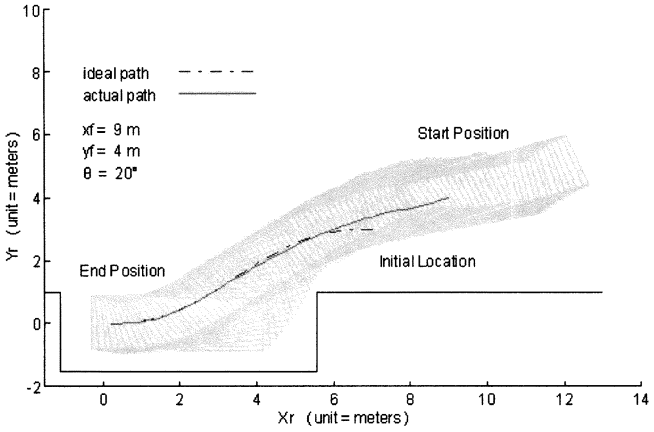

Fig. 15. Simulation result of backward parallel parking: vehicle with start posture $(x_{r2}, y_{r2}, \theta_2) = (9, 4, 20^\circ)$.

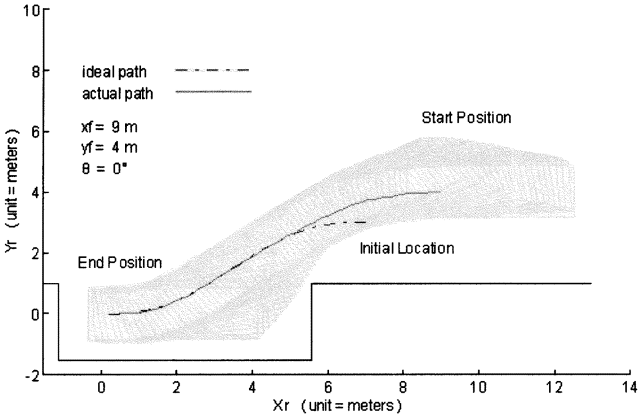

Fig. 16. Simulation result of backward parallel parking: vehicle with start posture $(x_{r2}, y_{r2}, \theta_2) = (9, 4, 0^\circ)$.

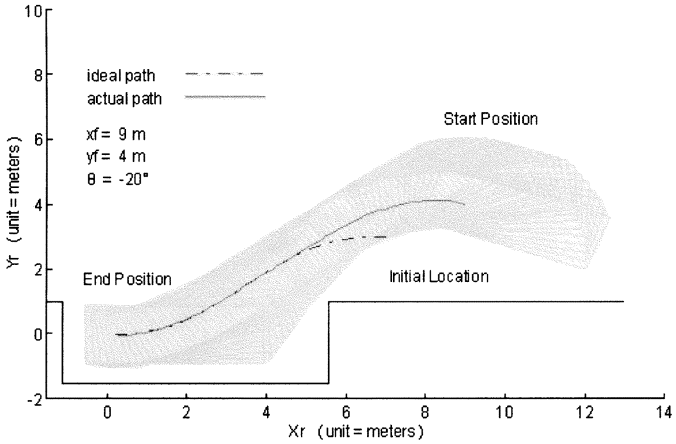

Fig. 17. Simulation result of backward parallel parking: vehicle with start posture $(x_{r2}, y_{r2}, \theta_2) = (9, 4, -20°)$.

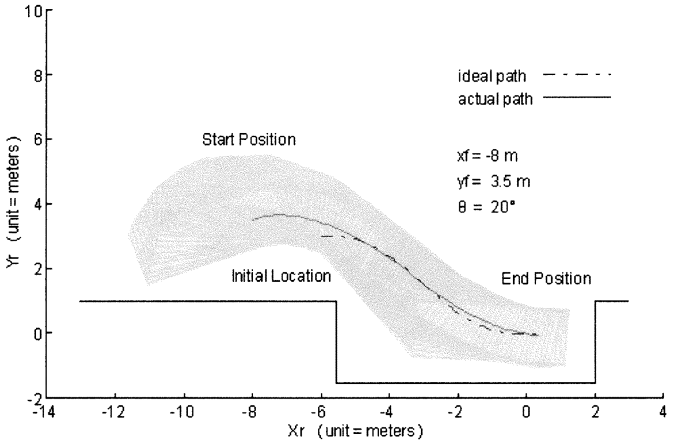

Fig. 18. Simulation result of forward parallel parking: vehicle with start posture $(x_{f2}, y_{f2}, \theta_2) = (-8, 3.5, 20°)$.

the following three cases to demonstrate the effectiveness of the proposed FPPC scheme. For backward parallel parking, the reference trajectory starts with the initial location $(x_e, y_e) = (7, 3)$ with orientation 0° and ends at the final location (0, 0) with orientation 0°. Suppose the start postures of the CLMR are respectively located at $(x_{r2}, y_{r2}, \theta_2) = (9, 4, 20°)$, (9, 4, 0°), (9, 4, $-20°$), Simulation results for these three start postures are illustrated in Figs. 15, 16, and 17, respectively.

For forward parallel parking, we also test the feasibility of the fuzzy logic controller via following three cases. The reference trajectory starts with the initial location $(x_e, y_e) = (-6, 3)$ with orientation 0° and ends at the final location (0, 0) with orientation 0°. If the start postures of the CLMR are respectively placed at $(x_{f2}, y_{f2}, \theta_2) = (-8, 3.5, 20°)$, (− 8, 3.5, 0°), and (− 8, 3.5, $-20°$), then the corresponding simulation trajectories for these three start postures are shown in Figs. 18, 19, and 20.

Note that the CLMR follows this reference trajectory and parks in the lot perfectly. We can also find that the less differences between the initial posture of the reference trajectory and the start posture of the CLMR, the less differences between the ides path and the actual path.

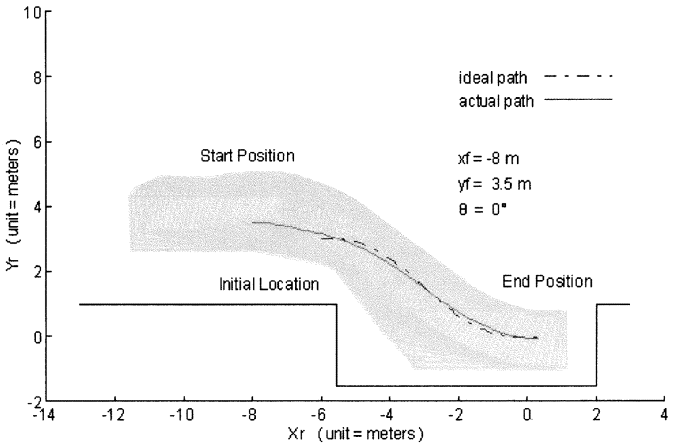

Fig. 19. Simulation result of forward parallel parking: vehicle with start posture $(x_{f2}, y_{f2}, \theta_2) = (-8, 3.5, 0°)$.

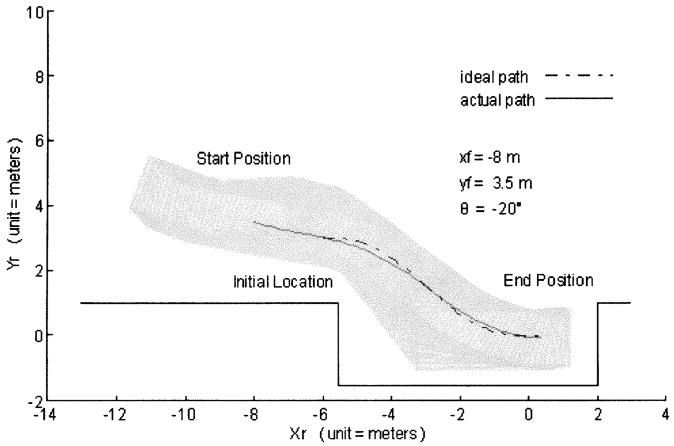

Fig. 20. Simulation result of forward parallel parking: vehicle with start posture $(x_{f2}, y_{f2}, \theta_2) = (-8, 3.5, -20°)$.

IV. Real-Time Fuzzy Parking Control Experiments

The fuzzy parking control mentioned in previous section is implemented in this section. The overall experimental setup of the parking system shown in Fig. 21 is composed of a host computer, a communication module, a CLMR, and a vision system. To implement the fuzzy parking control for the CLMR by vision system, a CCD camera is put above the working environment. At first, the CCD camera catches the image of the working environment. The host computer captures the image information via the grabber card. After image processing, the host computer calculates the posture (posture means both the position and the orientation of the CLMR) of the CLMR. The control scheme generates actions to maneuver the motion of the CLMR. The host computer sends commands (i.e. orientation and speed) to the CLMR via wireless radio modem. The CLMR receives commands via wireless radio modem and executes motion control commands. The flow chart of the system architecture is shown in Fig. 22. It consists of the following four parts, host computer, communication module, CLMR, and vision system. We describe the system architecture in the following subsection. By the way, the actual real-time experiments for backward garage-parking, forward garage-parking, backward parallel-parking, and forward parallel-parking tasks are also illustrated.

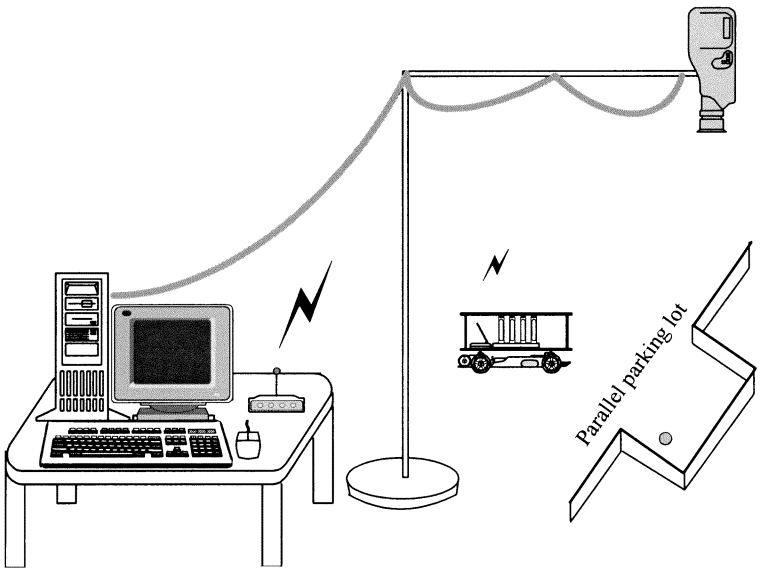

Fig. 21. Overview of the experimental setup.

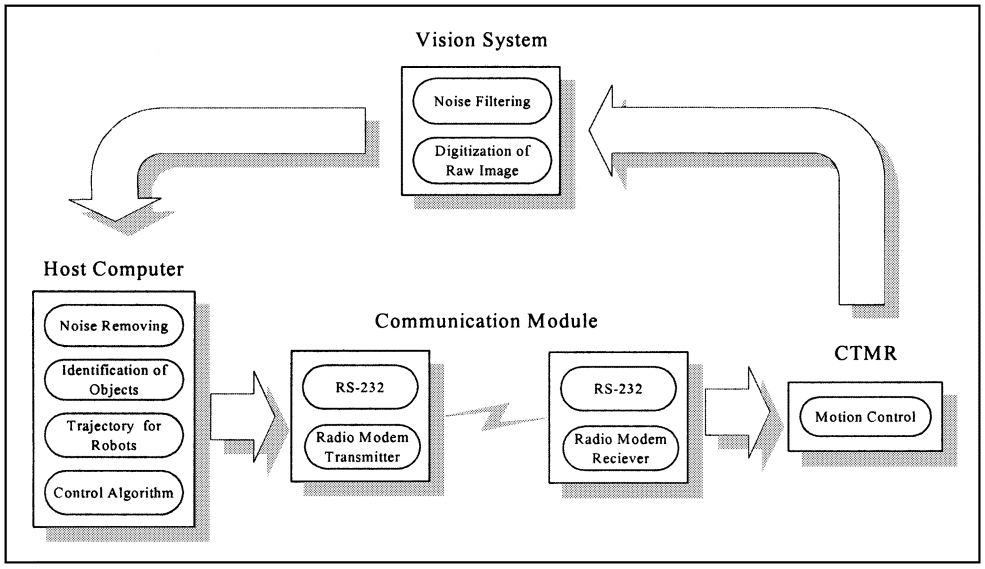

Fig. 22. Flow chart of the system architecture.

A. Host Computer

The specification of the host computer adopted here is the AMD Thunderbird 900M Hz with 256M SRAM, where the Meteor grabber card is equipped. The Meteor manufactured by Matrox Electronic Systems Ltd is adept at real-time grabbing image data and transmits the image data to external interface or displayed RAM. The Meteor comes with the software development kit, which includes the MIL (Matrox Imaging Library) and Matrox Intellicam. The kit is a C development library with commands for image acquisition, transfer, display control, and image processing applications. We can solve the intractable and time- consuming questions about image processing by using MIL functions.

B. Communication Module

SST-900 wireless radio modem used here is developed by ICP DAS as the communication media between the host computer and the CLMR. It can be used in the multiple access networking, and operating in 902–928 MHz based on direct sequence spread spectrum and RF technology. Fig.23(a) shows the appearance of SST-900. The SST-900 consists of one CPU, one spread spectrum technology chip, and one RF module [see Fig. 23(b)]. The SST-900 can operate in full-duplex or half-duplex mode and can handle the communication information in either synchronous or asynchronous way. Taking our requirements into account, our wireless modems are set as synchronous way, full-duplex mode and 4800 Baud rate. By using synchronous way, the CPU of SST-900 will operate sequentially the information with the fixed format as start bit (1 bit), information (8 bits), and stop bit (1 bit), therefore all of the SST-900 must be working in the same baud rate and information format. By using full-duplex mode, one SST-900 is master and transmits information, the other is slave and receives information from Master. Fig. 24 shows the SST-900 and RS-232 pin connection.

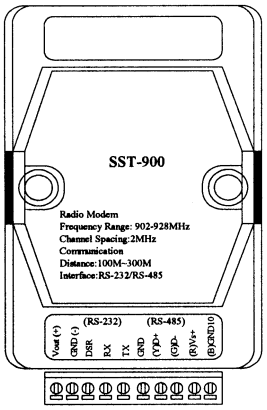

(a)

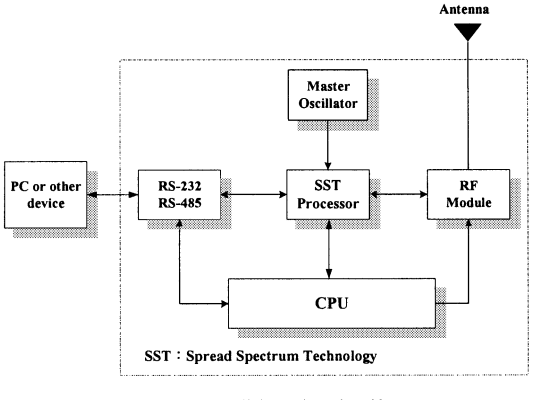

(b)

Fig. 23. (a) Appearance and (b) block diagram of SST-900.

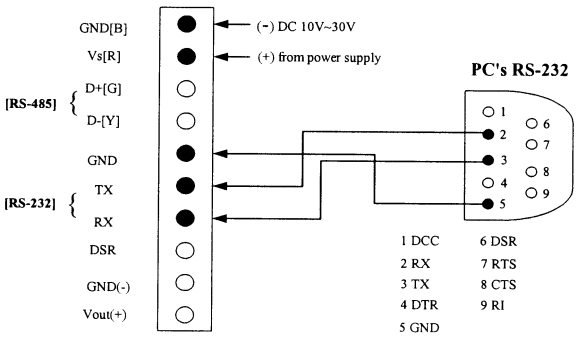

Fig. 24. Wire connection of PC's RS-232 to SST-900.

C. CLMR

The hardware architecture of the CLMR consists of the following four parts, CLMR mechanism, microcomputer module, A/D-D/A module, and electronic driver module. The mobile robot mechanism manufactured by TAMIYA Co. Ltd includes car body, driving motor, steering structure, gear trains, and transmission systems. A 1/10th scale mobile robot mechanism adopted here is a four-wheeled vehicle with front wheel drive and front steering wheels just like its full-size counterpart. The mobile robot carries the CPU board, A/D-D/A card, wireless radio modem, and so on. The appearance of the real autonomous CLMR is shown in Fig. 25. The signal processing block diagram of a CLMR is shown in Fig. 26.

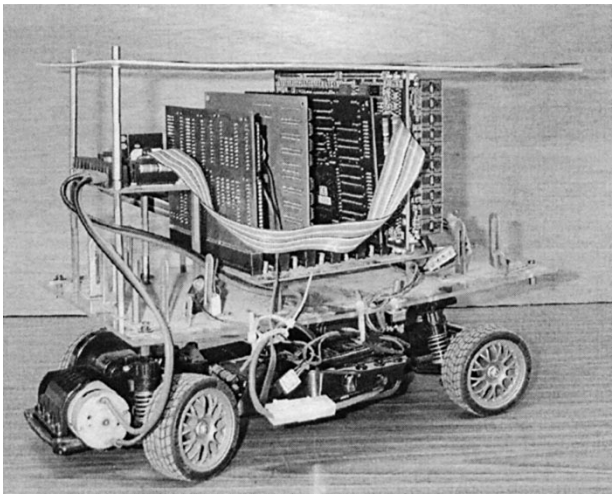

Fig. 25. Appearance of the CLMR.

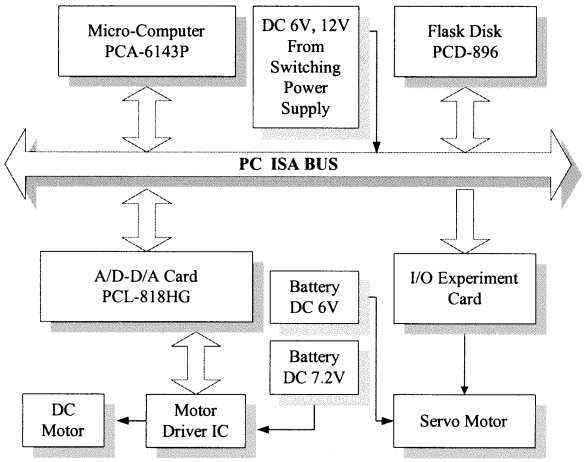

Fig. 26. Signal processing diagram of the CLMR.

The microcomputer module includes CPU board, and booting board. The CPU board (PCA-6143P), which is manufactured by Advantech Co. Ltd., is based on a 32 bit Intel 80 586DX4-100 CPU. The booting disk (PCD-896) manufactured by M-SYSTEMS flash disk Pioneers Ltd emulates a floppy disk drive by using solid-state memory chip to store program and data instead of the magnetic particles on the mechanical drive's disk. Hence, flash disk is installed as a bootable device.

The A/D-D/A module (PCL-818HG) manufactured by Advantech Co., Ltd acts a very important part in this control system. It offers five most desired measurements and control functions: 12 bits A/D conversion, D/A conversion, digital input, digital output and timer/counter. We control the speed of the DC motor via connected the D/A conversion of A/D-D/A module with TA7291P IC, and connect digital output of the A/D-D/A module with TA7291P IC for controlling the rotating direction of the DC motor.

The electronic driver module consists of a TA7291P DC motor driver IC and an I/O experiment card. The TA7291P IC is assembled in a PCB board to drive the DC motor to change

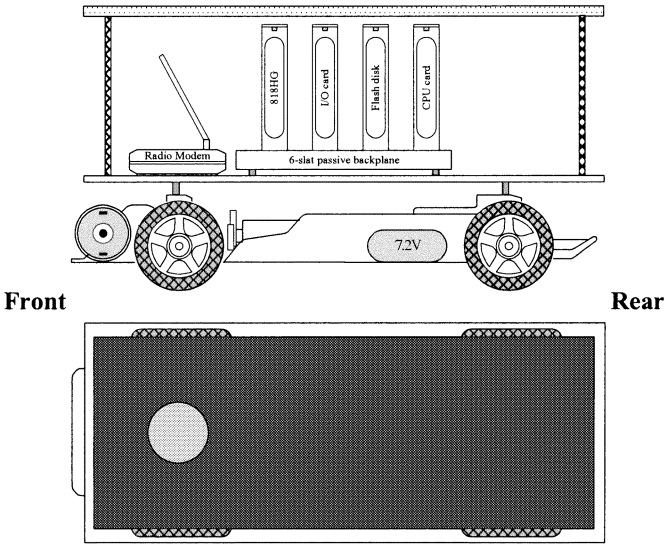

Fig. 27. Microcomputer system arrangement.

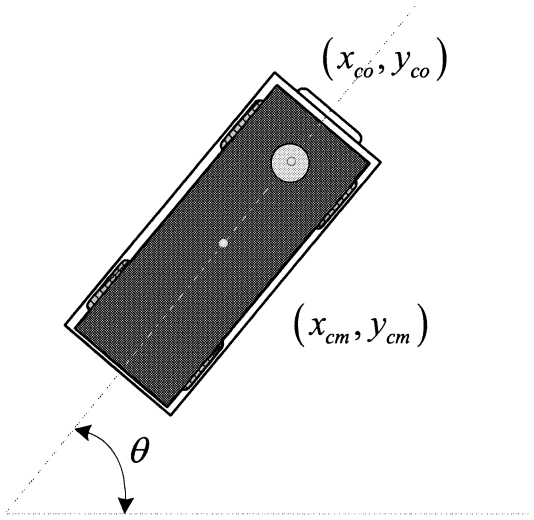

Fig. 28. Posture of the CLMR.

the speed of the front wheels. The I/O experiment card is manufactured by ICC Information Co., Ltd. We employ the I/O card to generate PWM signal and to drive the DC servomotor to control the steering angle of the front wheels. The microcomputer system arrangement is illustrated in Fig. 27. For recognizing the posture of the CLMR, a solid circle in orange color is used within a black board at the front wheel center above the CLMR in forward parking problem, and at the rear wheel center above the CLMR in backward parking problem.

D. Vision System

The image processing begins from CCD camera capture, the information of the working environment transmits host computer via Meteor grabber card. Each frame captured by the Meteor grabber card from CCD camera at each sampling has 640×480 pixels and each pixel has three eight-bit-depth color channels (red, green, and blue). We use HITACHI CCD color camera to photograph the image. The series number of the CCD is VK-C77U, and it uses DSP (Digital Signal Processing) technology to deal with the incoming image. We adopt the image-based visual servoing method [27] and [28], where the postures of objects in the image plane captured by the camera are not transformed into the Cartesian coordinate system.

In the vision-based system, image processing should have the capabilities to do some processing on strategies as well as for eliminating noise of the environment and calculating location of the CLMR. The color information of the environment can make the detection easier than gray level detection or an edge detection method. Specially, if the target object has a certain uniform color, we can easily calculate the position of the target object from the environment by the color information.

Using the RGB color model is an uncomplicated method, but it makes the detection sensitive to the environment conditions such as illumination. To solve this problem, the detection method must be improved by using HSI color model. The detection algorithm used here is a pixel search method. If pixels of environment are satisfying the HSI values of orange color, then the X and Y coordinate values of the pixel are summarized and the counter is increased by 1. After searching, the averages of X and Y summations are calculated by dividing the counter. The position of the CLMR is got and the direction of the CLMR is obtained by comparing with previous position of the CLMR. To eliminate the environment noise, an appropriate recognition method is required. For example, if some orange pixels are far away from the orange cluster, they are regarded as the environment noises. The down sampling is utilized for reducing the processing time.

Before the CLMR starts the parking missions, we will detect and calculate the location of the end position. We put a color mask in the end position and use the color detection method to calculate this position. As the CLMR is put on the experimental ground, we can know the start position of the CLMR. Then we can determine the reference trajectories from (9), (10) (16), and (18). In our experiments, the posture of the CLMR has to be known by image information. We should have an effective image recognition method to figure out the posture, which can be determined by the following two steps.

It is known that the MIL library offers an edge detection function to perform the edge detection operation and produce a gradient intensity. We first utilize this function to get the positions of four corners of the CLMR. By averaging these positions, one can obtain the center position of the CLMR, (x_{cm}, y_{cm}), as shown in Fig. 28. Second, we use the recognition method mentioned previously to find out the center position of the orange color circle, $x_{co}, y_{co})$. Thus, the direction of the CLMR can be calculated by $(x_{co} - x_{cm}, y_{co} - y_{cm})$. And the orientation θ of the vehicle can be obtained by

$$\theta = \tan^{-1} \frac{y_{co} - y_{cm}}{x_{co} - x_{cm}}. \tag{22}$$

After obtaining the posture of the CLMR, the host computer will compare it with the reference trajectory and then sent the control command to the CLMR. The CLMR will track the reference trajectory till it appropriately finishes the parking task.

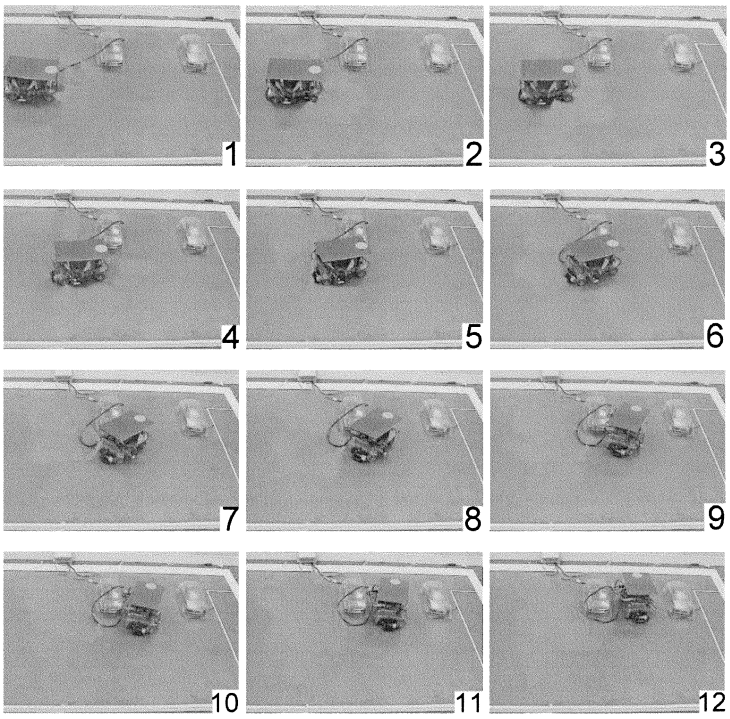

Fig. 29. Twelve sequential image stills of backward garage parking (captured by a handheld CCD camera).

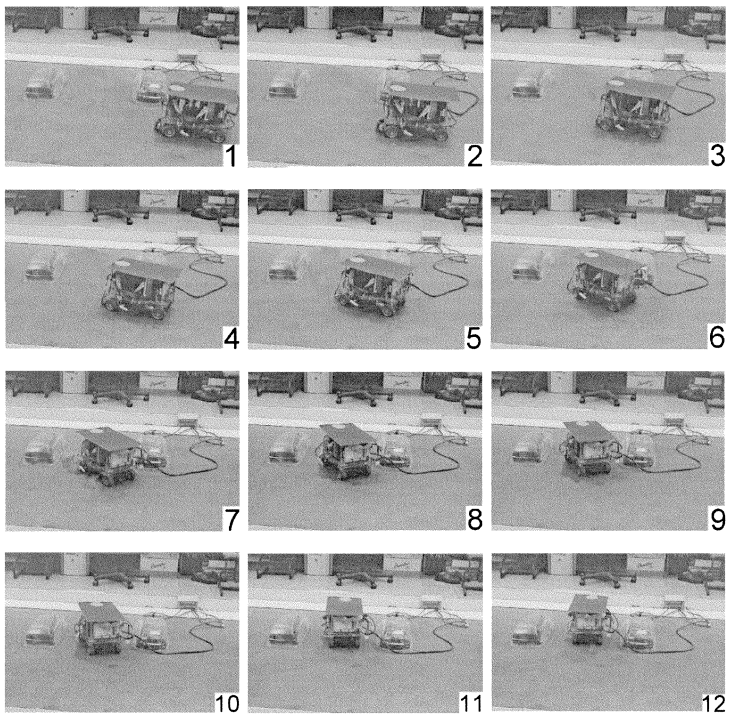

Fig. 30. Twelve sequential image stills of forward garage parking (captured by a handheld CCD camera).

E. Real-Time Experiments

Since the simulation results are successful, we want to use the developed CLMR to realize the FGPC schemes and the FPPC schemes. The established CLMR is shown in Fig. 25, its corresponding dimensions are length 380 mm, width 240 mm and weight 5 kg. For backward garage parking and forward garage parking, the dimensions of the garage are length 570 mm and width 360 mm, and length 570 mm and width 480 mm, respectively. For backward parallel parking and forward parallel parking, the dimensions of the parking zone are length 570 mm and width 360 mm, and length 760 mm and width 360 mm, respectively.

The actual experimental photographs for backward garage-parking, forward garage-parking, backward parallel-parking,

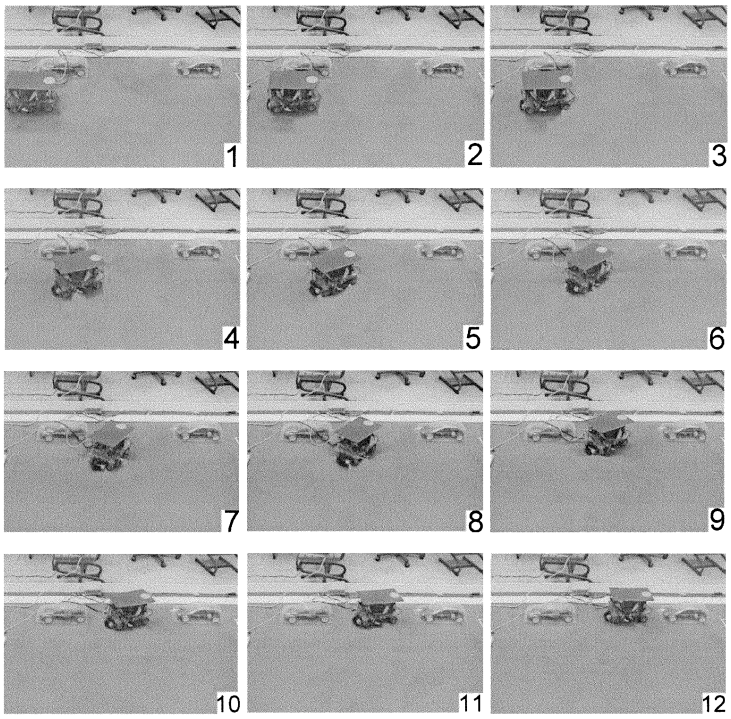

Fig. 31. Twelve sequential image stills of backward parallel parking (captured by a handheld CCD camera).

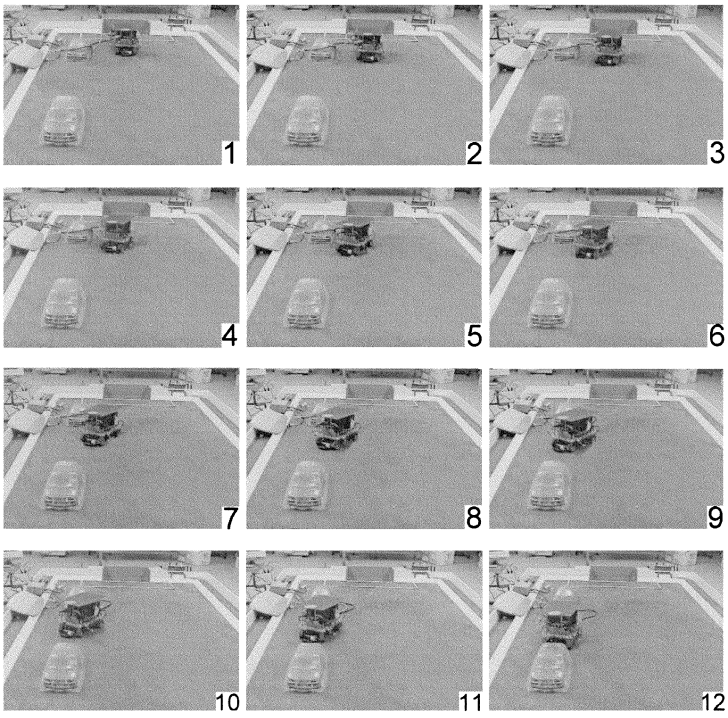

Fig. 32. Twelve sequential image stills of forward parallel parking (captured by a handheld CCD camera).

and forward parallel-parking tasks are demonstrated in Figs. 29, 30, 31, and 32, respectively. One can find that the proposed FLC schemes can successfully accomplish the parking missions.

V. Conclusion

In this paper, we have designed and implemented an autonomous CLMR control system, where the host computer, communication module, CLMR, and vision system, have been set up. The host computer captures the working environment via the vision system, and calculates the posture of the CLMR by utilizing image processing. The host computer sends commands to the CLMR via wireless radio modem. The CLMR receives commands via wireless radio modem and executes motion commands. No matter forward or backward driving, we have introduced the reference trajectories for garage parking

and parallel parking, respectively. We also have proposed two FGPC schemes and two FPPC schemes, respectively. All computer simulations and practically experimental results illustrate that the propounded FGPC and FPPC methods are indeed effective and feasible.

ACKNOWLEDGMENT

The authors are grateful to the anonymous reviewers for their valuable comments, which improved the contents of this paper considerably.

REFERENCES

[1] M. Sugeno and K. Murakami, "An experimental study on fuzzy parking control using a model car," in *Industrial Applications of Fuzzy Control*, M. Sugeno, Ed. North-Holland, The Netherlands, 1985, pp. 105–124.
[2] M. Sugeno, T. Murofushi, T. Mori, T. Tatematsu, and J. Tanaka, "Fuzzy algorithmic control of a model car by oral instructions," *Fuzzy Sets Syst.*, vol. 32, pp. 207–219, 1989.
[3] A. Ohata and M. Mio, "Parking control based on nonlinear trajectory control for low speed vehicles," in *Proc. IEEE Int. Conf. Industrial Electronics*, 1991, pp. 107–112.
[4] S. Yasunobu and Y. Murai, "Parking control based on predictive fuzzy control," in *Proc. IEEE Int. Conf. Fuzzy Systems*, vol. 2, 1994, pp. 1338–1341.
[5] W. A. Daxwanger and G. K. Schmidt, "Skill-based visual parking control using neural and fuzzy networks," in *Proc. IEEE Int. Conf. System, Man, Cybernetics*, vol. 2, 1995, pp. 1659–1664.
[6] A. Tayebi and A. Rachid, "A time-varying-based robust control for the parking problem of a wheeled mobile robot," in *Proc. IEEE Int. Conf. Robotics and Automation*, 1996, pp. 3099–3104.
[7] M. C. Leu and T. Q. Kim, "Cell mapping based fuzzy control of car parking," in *Proc. IEEE Int. Conf. Robotics Automation*, 1998, pp. 2494–2499.
[8] H. An, T. Yoshino, D. Kashimoto, M. Okubo, Y. Sakai, and T. Hamamoto, "Improvement of convergence to goal for wheeled mobile robot using parking motion," in *Proc. IEEE Int. Conf. Intelligent Robots Systems*, 1999, pp. 1693–1698.
[9] B. Shirazi and S. Yih, "Learning to control: a heterogeneous approach," in *Proc. IEEE Intl. Symp. Intelligent Control*, 1989, pp. 320–325.
[10] M. Ohkita, H. Mitita, M. Miura, and H. Kuono, "Traveling experiment of an autonomous mobile robot for a flush parking," in *Proc. 2nd IEEE Conf. Fuzzy System*, vol. 2, Francisco, CA, 1993, pp. 327–332.
[11] D. Lyon, "Parallel parking with curvature and nonholonomic constraints," in *Proc. Symp. Intelligent Vehicles*, Detroit, MI, 1992, pp. 341–346.
[12] R. M. Murray and S. S. Sastry, "Nonholonomic motion planning: steering using sinusoids," *IEEE Trans. Automat. Contr.*, vol. 38, pp. 700–716, May 1993.
[13] J. P. Laumond, P. E. Jacobs, M. Taix, and R. M. Murray, "A motion planner for nonholonomic mobile robots," *IEEE Trans. Robot. Automat.*, vol. 10, pp. 577–593, Oct. 1994.
[14] I. E. Paromtchik and C. Laugire, "Motion generation and control for parking an autonomous vehicle," in *Proc. IEEE Conf. Robotics Automation*, vol. 4, Minneapolis, MN, 1996, pp. 3117–3122.
[15] C. Laugier, T. Fraichard, I. E. Paromtchik, and P. Garnier, "Sensor-based control architecture for a car-like vehicle," in *Proc. IEEE Int. Conf. Intelligent Robots Systems*, 1998, pp. 216–222.
[16] D. Leitch and P. J. Probert, "New techniques for genetic development of a class of fuzzy controllers," *IEEE Trans. Syst., Man, Cybern. C*, vol. 28, pp. 112–123, Feb. 1998.
[17] L. Dorst, "Analyzing the behaviors of a car: a study in abstraction of goal-directed motions," *IEEE Trans. Syst., Man, Cybern. A*, vol. 28, pp. 811–822, Nov. 1998.
[18] K. Y. Lian, C. S. Chin, and T. S. Chiang, "Parallel parking a car-like robot using fuzzy gain scheduling," in *Proc. 1999 IEEE Int. Conf. Control Applications*, vol. 2, 1999, pp. 1686–1691.
[19] K. Jiang and L. D. Seneviratne, "A sensor guided autonomous parking system for nonholonomic mobile robots," in *Proc. IEEE Int. Conf. Robotics Automation*, vol. 1, 1999, pp. 311–316.
[20] K. Jiang, "A sensor guided parallel parking system for nonholonomic vehicles," in *Proc. IEEE Conf. Intelligent Transportation Systems*, 2000, pp. 270–275.
[21] J. Xiu, G. Chen, and M. Xie, "Vision-guided automatic parking for smart car," in *Proc. IEEE Intelligent Vehicles Symp.*, 2000, pp. 725–730.
[22] D. Gorinevsky, A. Kapitanovsky, and A. Goldenberg, "Neural network architecture for trajectory generation and control of automated car parking," *IEEE Trans. Contr. Syst. Technol.*, vol. 4, pp. 50–56, Jan. 1996.
[23] S. Lee, M. Kim, Y. Youm, and W. Chung, "Control of a car-like mobile robot for parking problem," in *Proc. IEEE Int. Conf. Robotics Automation*, 1999, pp. 1–6.
[24] C. S. Ting, T. H. S. Li, and F. C. Kung, "An approach to systematic design of the fuzzy control system," *Fuzzy Sets Syst.*, vol. 77, pp. 151–166, 1996.
[25] T. H. S. Li and M. Y. Shieh, "Switching-type fuzzy sliding mode control of a cart-pole system," *Mechatronics*, vol. 10, pp. 91–109, 2000.
[26] O. Kaynak, K. Erbatur, and M. Ertugrul, "The fusion of computationally intelligent methodologies and sliding-mode control—a survey," *IEEE Trans. Ind. Electron.*, vol. 48, pp. 4–17, Feb. 2001.
[27] S. Hutchinson, G. D. Hager, and P. I. Corke, "A tutorial on visual servo control," *IEEE Trans. Robot. Automat.*, vol. 12, pp. 651–669, Oct. 1996.
[28] J. S. Cho, H. W. Kim, and I. S. Kweon, "Image-based visual servoing using position and angle of image features," *Electron. Lett.*, vol. 37, pp. 208–214, 2001.

Tzuu-Hseng S. Li (S'85–M'90) received the B.S. degree in 1981 from Ta-Tung Institute of Technology, Taipei, Taiwan, R.O.C., and the M.S. and Ph.D. degrees in 1985, from National Cheng-Kung University (NCKU), Tainan, Taiwan, all in electrical engineering.

He has been a Professor in the Department of Electrical Engineering, NCKU since 1994. He has served as a Researcher for the Engineering and Technology Promotion Center of the National Science Council since 1996. From 1999 to 2002, he served as a Director of Electrical Laboratories, NCKU. His current research interests include singular perturbation, intelligent control IC and system, mechatronics, mobile robots, RoboCup, and automobile active suspension systems.

Shih-Jie Chang received the B.S. degree in electrical engineering from Chung Yuan Christian University, Chung-Li, Taiwan, R.O.C. and the M.S. degree in electrical engineering from National Cheng Kung University (NCKU), Tainan, Taiwan, in 1995 and 1997, respectively. He is currently working toward the Ph.D. degree in the Department of Electrical Engineering, NCKU, Tainan, Taiwan, R.O.C.

His current research interests are concerned with fuzzy logic control, intelligent control, and mobile robots.